Enhanced regular perturbation-based nonlinearity compensation technique for optical transmission systems

Please check the document version of this publication:

• A submitted manuscript is the version of the article upon submission and before peer-review. There can be important differences between the submitted version and the official published version of record. People interested in the research are advised to contact the author for the final version of the publication, or visit the DOI to the publisher's website.
• The final author version and the galley proof are versions of the publication after peer review.
• The final published version features the final layout of the paper including the volume, issue and page numbers.

Link to publication

Enhanced Regular Perturbation-Based Nonlinearity Compensation Technique for Optical Transmission Systems

O. S. Sunish Kumar, *Student Member, IEEE*
Abdelkerim Amari, *Member, IEEE*
Octavia A. Dobre, *Senior Member, IEEE*
Ramachandran Venkatesan, *Life Senior Member, IEEE*
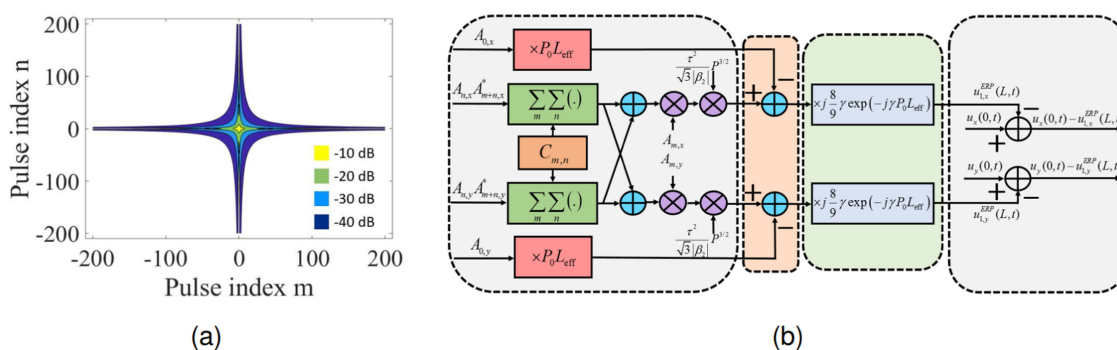
(a)　　　　　　　　　　　　　　　　(b)

Enhanced Regular Perturbation-Based Nonlinearity Compensation Technique for Optical Transmission Systems

O. S. Sunish Kumar [ORCID],[1] *Student Member, IEEE,*
Abdelkerim Amari [ORCID],[2] *Member, IEEE,*
Octavia A. Dobre [ORCID],[1] *Senior Member, IEEE,*
and Ramachandran Venkatesan [ORCID],[1] *Life Senior Member, IEEE*

[1]Faculty of Engineering and Applied Science, Memorial University, St. Johns, NL A1B 3X5, Canada
[2]Signal Processing Systems Group, Eindhoven University of Technology, 5612 AZ Eindhoven, The Netherlands

Abstract: The regular perturbation (RP) series used to analytically approximate the solution of the nonlinear Schrodinger equation has a serious energy-divergence problem when truncated to the first order. The enhanced RP (ERP) method can improve the accuracy of the first-order RP approximation by solving the energy divergence problem. In this paper, we propose an ERP-based nonlinearity compensation technique, referred to as ERP-NLC, to compensate for the fiber nonlinearity in a polarization-division multiplexed dispersion unmanaged optical communication system. We also propose a modified perturbation-based NLC (PB-NLC) technique by simple phase-rotation (PR) of the nonlinear coefficient matrix, referred to as the PR-PB-NLC. The PR-PB-NLC can be considered as a by-product of the ERP-NLC technique. We show through numerical simulation that, for a 256 Gb/s single-channel system, the proposed ERP-NLC technique improves the *Q*-factor performance by ∼1.2 dB and ∼0.6 dB when compared to the electronic dispersion compensation (EDC) and the PB-NLC techniques, respectively, at a transmission distance of 2800 km. Also, the result for a 1.28 Tb/s wavelength-division multiplexed five-channel transmission system at the same transmission distance shows that the *Q*-factor performance of the ERP-NLC technique is improved by ∼0.6 dB and ∼0.4 dB when compared to the EDC and the PB-NLC techniques, respectively. The simulation results for the PR-PB-NLC technique for a single- or five-channel transmission system show an improved *Q*-factor performance when compared to the EDC and PB-NLC techniques. Finally, we show that the proposed performance enhancement comes with a negligible increase in the computational complexity for the ERP-NLC and PR-PB-NLC techniques when compared to the PB-NLC technique.

Index Terms: Coherent detection, enhanced perturbation, fiber nonlinearity, optical communications.

1. Introduction

The intra-channel fiber nonlinearity effect is considered a dominant impairment in a dispersion unmanaged optical communication system [1]–[3]. However, the deterministic nature of intra-channel nonlinearity allows its electronic compensation either at the transmitter as a pre-compensation, or at the receiver as post-compensation [4]. That is enabled by the introduction of coherent

detection and advances in the digital signal processing technology. Digital back-propagation (DBP) is a widely investigated nonlinearity compensation (NLC) technique to combat the detrimental effects of fiber nonlinearity [5]. DBP can compensate both dispersion and deterministic intra-channel nonlinearity based on a numerical solution of the nonlinear Schrodinger equation (NLSE) using the split-step Fourier method (SSFM) [5]. SSFM involves a large number of linear and nonlinear computation steps per fiber span, thereby the practical implementation of DBP is limited [4]. That led to increased interest in research for the NLC techniques based on the simplified versions of the NLSE for which an approximate analytical solution is available. As a result, a Volterra series-based nonlinear equalizer (VNLE) has been proposed in [6]–[8] to compensate for fiber nonlinearity. On the other hand, when applied to long-haul optical fiber links, the computational complexity of the VNLE may approach that of the DBP technique [4].

In contrast to the VNLE, the first-order regular perturbation (RP) theory-based NLC referred to as PB-NLC, has been proposed in the literature to compensate for the fiber nonlinearity effects [9]–[12]. The PB-NLC technique exhibits reduced computational complexity in comparison with DBP and VNLE. The first-order RP theory was initially used to model the intra-channel nonlinear distortion effects between short and highly dispersive Gaussian pulses propagating in single-polarization optical fiber links [13]. This technique was later extended to dual-polarization systems and applied as a low-complexity digital NLC in [14]. It is important to note that the first-order RP theory adopted in the PB-NLC technique has a serious energy divergence problem when the fiber launch power increases [15]. That is due to the inaccuracy of the first-order RP series approximation for the nonlinear phase-shift. To solve this issue, an enhanced RP (ERP) method was proposed in [15], to model the nonlinear signal propagation in the optical fiber. The ERP method employs a change of variable technique to eliminate the average cumulated nonlinear phase, around which the phase of the received signal field swings, before applying the RP method [15]. The ERP-based technique was initially proposed to model the nonlinearity in dispersion-managed systems [15]. Later, in [16], the ERP approach was adopted for an alternative framework to derive the well-known Gaussian noise reference formula in time-domain to model the nonlinear signal propagation in dispersion unmanaged systems. The ERP method improves the accuracy of the first-order RP solution at the power levels of interest in dispersion unmanaged long-haul transmission systems.

In this paper, we propose to use an ERP-based method to compensate for the intra-channel nonlinearity, referred to as the ERP-NLC technique. We also introduce a technique, which is a by-product of the ERP-NLC, by simple phase-rotation (PR) of the nonlinear coefficient matrix of the PB-NLC technique, referred to as the PR-PB-NLC. The main contributions of this work are as follows. First, we provide a generalized description to show that the ERP technique can solve the energy divergence problem of the RP-based approach in a dispersion unmanaged transmission system. Second, we derive the first-order ERP distortion field in time-domain with Gaussian shape assumption for the input pulses, and third, we develop the nonlinear coefficient matrix of the PR-PB-NLC technique by considering only a part of the first-order ERP distortion field. We carried out numerical simulations for a single and five-channel polarization division multiplexed 16-quadrature-amplitude-modulation (QAM) optical transmission system. The results show that the proposed ERP-NLC technique provides a significant performance improvement in terms of the Q-factor and transmission reach, with only a negligible increase in the computational complexity, when compared to the PR-PB-NLC, PB-NLC, and electronic dispersion compensation (EDC) techniques. Furthermore, we show that the performance improvement of the PR-PB-NLC technique also comes with a negligible additional computational complexity when compared to the PB-NLC technique.

This paper is organized as follows. Section 2 provides a detailed theory on the ERP-based approximation of the NLSE and the principle of the proposed ERP-NLC technique. Section 3 explains the simulation setup, and Section 4 discusses results for the ERP-NLC and PR-PB-NLC techniques. Section 5 presents the complexity evaluation, and Section 6 concludes the paper. Appendix A provides the detailed derivation of the first-order ERP-based distortion field, and Appendix B considers it's dual polarization extension.

2. Principle of ERP-Based NLC

2.1 The ERP-Based Approximation of the NLSE

In this section, we provide a generalized description to show the effectiveness of the ERP method in solving the energy divergence problem of the RP-based approximation for a dispersion unmanaged transmission system. It is important to note that the demonstration with a zero-dispersion fiber given in [15] can be considered as a special case of our generalized description. The NLSE that describes the evolution of the optical field envelope through an optical fiber is represented as [17]:

$$\frac{\partial}{\partial z} q(z, t) + \frac{\alpha}{2} q(z, t) + j\frac{\beta_2}{2}\frac{\partial^2}{\partial t^2} q(z, t) = j\gamma \left| q(z, t) \right|^2 q(z, t), \tag{1}$$

where $q(z, t)$ is the optical field, t is the time variable, z is the transmission distance, α is the attenuation, β_2 is the group velocity dispersion, and γ is the nonlinearity coefficient.

The NLSE in (1) can be further simplified by applying the transformation $q(z, t) \triangleq u(z, t) \exp(-\frac{\alpha}{2}z)$, referred to the delayed time frame $t = \hat{t} - (z/v_g)$ corresponding to the group velocity v_g, and separating the linear and nonlinear parts as [15], [18]:

$$\frac{\partial}{\partial z} u(z, t) = \left(\hat{D} + \hat{N} \right) u(z, t) \tag{2}$$

$$\hat{D} = -j\frac{\beta_2}{2}\frac{\partial^2}{\partial t^2} \tag{3}$$

$$\hat{N} = j\gamma \left| u(z, t) \right|^2 \exp(-\alpha z), \tag{4}$$

where $\hat{D}$ and $\hat{N}$ are the linear and nonlinear operators [18]. The simplified NLSE in (2) can be numerically solved using the symmetric SSFM as given in [18]. For a special case of $z = z'$ (i.e., the first computation step) the symmetric SSFM yields the solution:

$$u^{SSFM}(z', t) = \exp\left(\frac{z'}{2}\hat{D}\right) \exp\left(\int_0^{z'} \hat{N}(z)dz\right) \exp\left(\frac{z'}{2}\hat{D}\right) u(0, t), \tag{5}$$

where z' is the step size. It is important to note that the SSFM preserves the energy if the step size is appropriately selected. The choice of the step size depends on the specific dispersive and nonlinear properties of the link, such as the dispersion length and the nonlinear length. The criteria for selecting the optimal step size that satisfies the conservation of energy is given in [19].

Alternatively, (2) can be analytically solved using the first-order RP method [15]. The RP-based approach is an iterative method which provides a closed-form approximate solution of the NLSE. The first-order RP approximation to the optical field after a transmission distance $z = z'$ (the step size in the SSFM) is given as:

$$u^{RP}(z', t) = u_0(z = z', t) + j\gamma \int_0^{z'} \exp(-\alpha z) \left(h_z(t) \otimes \left[\left| u_0(z, t) \right|^2 u_0(z, t) \right] \right) dz, \tag{6}$$

where $u_0(z, t) = [h_z(t) \otimes u(0, t)]$, is the linear (zeroth-order) solution, with $\otimes$ as the convolution operation, $h_z(t) = \mathcal{F}^{-1}\{\exp(-j\frac{w^2\beta_2 z}{2})\}$ at the angular frequency w, and $\mathcal{F}^{-1}\{.\}$ as the inverse Fourier transform (IFT) operation.

By closely inspecting (5), it can be seen that the signal power at a transmission distance $z = z'$ is $\left| u(0, t) \right|^2$, which is same as the input power at $z = 0$. On the other hand, the first-order RP series approximation in (6) overestimates the signal power at $z = z'$ and the relative error grows with increasing the launch power. To mitigate this discrepancy, the ERP method has been proposed in [15]. In the ERP method, a change of variable is applied in (2) to eliminate the cumulated nonlinear phase before applying the first-order RP method. The first step is to postulate the solution of (2) as [15]:

$$u(z, t) \triangleq \tilde{u}(z, t) \exp(-j\gamma P_0 L_{\text{eff}}), \tag{7}$$

where $L_{eff} \triangleq \int_0^z \exp(-\frac{\alpha}{2}\xi)d\xi$ is the fiber effective length and P_0 is the peak input power. Substituting (7) in (2) factors out the cumulated nonlinear phase from the solution. As a result, (2) with the field $\tilde{u}(z, t)$ and substituting the expressions for $\hat{D}$ and $\hat{N}$, we obtain [15]:

$$\frac{\partial}{\partial z}\tilde{u}(z, t) = -j\frac{\beta_2}{2}\frac{\partial^2}{\partial t^2}\tilde{u}(z, t) + j\gamma[|\tilde{u}(z, t)|^2 - P_0]\tilde{u}(z, t). \tag{8}$$

The next step is to solve (8) using the first-order RP method. Accordingly, from (7) and (8), the zeroth-order solution of the optical field at a transmission distance $z = z'$ is obtained as:

$$u_0^{ERP}(z', t) = \tilde{u}_0(z = z', t)\exp(-j\gamma P_0 L_{eff}), \tag{9}$$

where $\tilde{u}_0(z, t) = [h_z(t) \otimes \tilde{u}(0, t)]$. Similarly, the first-order ERP solution can be represented as:

$$u_1^{ERP}(z', t) = j\gamma \int_0^{z'} \exp(-\alpha z)\left(h_z(t) \otimes \left[\left(|\tilde{u}_0(z, t)|^2 - P_0\right)\tilde{u}_0(z, t)\right]\right) dz\, \exp(-j\gamma P_0 L_{eff}). \tag{10}$$

Combining (9) and (10), the analytical approximation to the optical field at a transmission distance $z = z'$ based on the first-order ERP series can be represented as:

$$u^{ERP}(z', t) \approx \tilde{u}_0(z', t)\exp(-j\gamma P_0 L_{eff})$$

$$+ j\gamma \int_0^{z'} \exp(-\alpha z)\left(h_z(t) \otimes \left[\left(|\tilde{u}_0(z, t)|^2 - P_0\right)\tilde{u}_0(z, t)\right]\right) dz\, \exp(-j\gamma P_0 L_{eff}). \tag{11}$$

From (11), it can be seen that the signal power at a transmission distance $z = z'$ is close to $|u(0, t)|^2$, especially when the input field magnitude approaches its peak value $\sqrt{P_0}$.

2.2 The ERP-NLC Technique

The time-domain nonlinear distortion field based on the first-order ERP method is obtained by solving (10) with Gaussian pulse shape assumption for the input pulses. Following the analysis given in Appendix A, the time-domain first-order distortion field at a transmission distance $z = L$ can be represented as:

$$u_1^{ERP}(L, t + kT) = j\gamma P^{3/2}\exp(-j\gamma P_0 L_{eff})\sum_m \sum_n \sum_l A_m A_n A_l^*$$

$$\times \exp\left(-\frac{t^2}{6\tau^2}\right)\int_0^L \frac{\exp(-\alpha z)}{\sqrt{1 + 2j\beta_2 z/\tau^2 + 3(\beta_2 z/\tau^2)^2}}$$

$$\underbrace{\times \exp\left\{-\frac{3\left[\frac{2}{3}t + (m-l)T\right]\left[\frac{2}{3}t + (n-l)T\right]}{\tau^2\left(1 + 3j\beta_2 z/\tau^2\right)} - \frac{(n-m)^2 T^2}{\tau^2\left[1 + 2j\beta_2 z/\tau^2 + 3(\beta_2 z/\tau^2)^2\right]}\right\} dz}_{\text{term 1}}$$

$$\underbrace{- j\gamma P_0 A_k \exp\left(-\frac{t^2}{2\tau^2}\right)\int_0^L \exp(-\alpha z)\exp(-j\gamma P_0 L_{eff})dz}_{\text{term 2}}, \tag{12}$$

where $k = m + n - l$, m, n, l are the symbol indices, P is the launch power, τ is the pulse width, and T is the symbol interval.

Equation (12) calculates the time-domain first-order ERP distortion field at $k = m + n - l$ caused by the nonlinear interaction between three pulses located at the time indices m, n, and l. Since the ERP technique is a modification to the RP method, we followed a similar mathematical analysis in [14] to derive the nonlinear distortion field. In term 1 of (12), we obtained a modified expression with a time-invariant phase-rotation term $\exp(-j\gamma P_0 L_{\text{eff}})$ when compared to the PB-NLC technique. On the other hand, term 2 is solely obtained in our analysis and is proportional to the complex amplitude of the symbol at time index k.

The basic idea of the ERP-NLC pre-compensation technique is to calculate the nonlinear distortion field using (12), and then to subtract it from the transmitted field to generate the pre-distorted waveform. In general, the integrals in (12) cannot be solved analytically due to the presence of the attenuation term. Therefore, we adopt the conventional RP method by ignoring $\exp(-\alpha z)$, as given in [13], to obtain the closed-form solution. Without loss of generality, in the implementation, we focus on the perturbation of the symbol at index $k = 0$, i.e., $l = m + n$. That will simplify (12) by replacing the triple summation with a double summation. It is worth mentioning that the nonlinear distortion field calculation at any other index, for example $k = m + n - l$, using (12) is the same as the calculation at $k = 0$. The pre-compensation is assumed to operate at the symbol rate; therefore, only the perturbation value at $t = 0$ is calculated. In a typical dispersion unmanaged optical transmission system, the chromatic dispersion-induced pulse spreading is usually much larger than the symbol duration, i.e., $\beta_2 z >> \tau^2$ [14]. With the large chromatic dispersion assumption and following a similar procedure as in [14], the nonlinear distortion field for the zeroth symbol at $t = 0$ can be obtained as:

$$u_1^{ERP}(L, t) = j\gamma \exp(-j\gamma P_0 L_{\text{eff}}) \left[\frac{\tau^2}{\sqrt{3}\,|\beta_2|} P^{3/2} \sum_m \sum_n A_m A^*_{m+n} A_n C_{m,n} - P_0 A_0 L_{\text{eff}} \right]. \qquad (13)$$

In (13), $C_{m,n}$ is the perturbation coefficient matrix, which is represented as:

$$C_{m,n} = \begin{cases} \int_0^L dz \frac{1}{\sqrt{\tau^4/(3\beta_2^2)+z^2}}, & m = n = 0 \\ \frac{1}{2}E_1\left(\frac{(n-m)^2 T^2 \tau^2}{3|\beta_2|^2 L^2}\right), & m \text{ or } n = 0 \\ E_1\left(-j\frac{mnT^2}{\beta_2 L}\right), & m \neq n \neq 0, \end{cases} \qquad (14)$$

where $E_1(x) = \int_x^\infty \frac{e^{-t}}{t} dt$ is the exponential integral function.

The nonlinear distortion field in (13) can be extended to dual polarization using the Manakov equation for the nonlinear signal propagation, as shown in Appendix B. Using (28) one can show that the six Gaussian input pulses $\sqrt{P} A_{m/l/n,x/y} \exp(-(t - T_{m/l/n})^2/2\tau^2)$ at three time instants T_m, T_l, T_n for the two polarizations generate the nonlinear distortion field for the zeroth symbol, i.e., $l = m + n$, as:

$$u_{1,x/y}^{ERP}(L, t) = j\frac{8}{9}\gamma \exp(-j\gamma P_0 L_{\text{eff}}) \left[\frac{\tau^2}{\sqrt{3}\,|\beta_2|} P^{3/2} \sum_m \sum_n (A_{n,x/y} A^*_{m+n,x/y} A_{m,x/y} \right.$$

$$\left. + A_{n,y/x} A^*_{m+n,y/x} A_{m,x/y}) C_{m,n} - P_0 A_{0,x/y} L_{\text{eff}} \right], \qquad (15)$$

where $A_{m/(m+n)/n,x/y}$ and $A_{0,x/y}$ are the symbol complex amplitudes. It is important to note that the peak power P_0 is selected as $\frac{3}{2}P$ in the implementation of the ERP-NLC technique, as per the analysis given in [16].

The first-order ERP-based nonlinear distortion field in (15) consists of a time-invariant phase rotation term $\exp(-j\gamma P_0 L_{\text{eff}})$ and a time-variant term proportional to the complex amplitude of the symbol at index 0, when compared to the RP-based distortion field in [14]. It is noteworthy that the perturbation coefficient matrix $C_{m,n}$ and the phase rotation term $\exp(-j\gamma P_0 L_{\text{eff}})$ are calculated offline and stored in look-up tables. As a result, the performance improvement of the proposed ERP-NLC technique comes with a negligible additional complexity when compared to the PB-NLC technique.
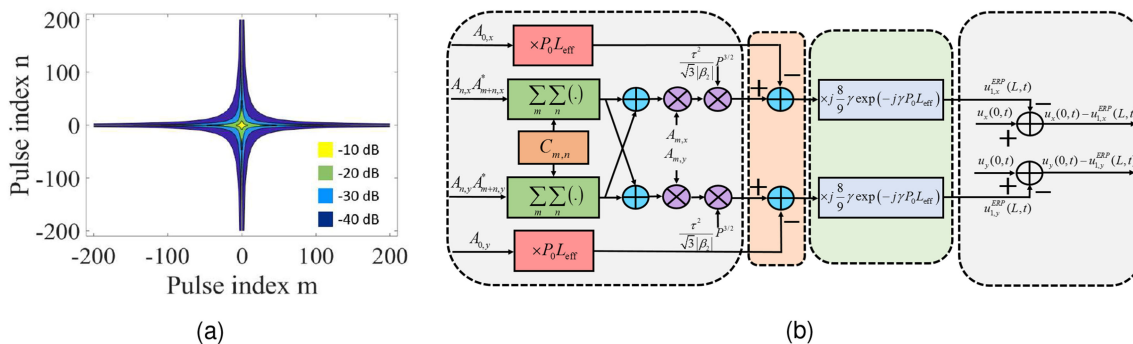
Fig. 1. (a) The magnitude of $C_{m,n}$ relative to the largest coefficient $C_{0,0}$, at a transmission distance of 1200 km and (b) the block diagram of the ERP-NLC technique.

Besides the ERP-NLC technique, we consider a method by simple PR of the perturbation coefficient matrix of the PB-NLC technique by using only the first part of (15). We refer to this technique as PR-PB-NLC. It is worth mentioning that the PR-PB-NLC is similar to an intra-channel NLC technique proposed in [20]. The method given in [20] modifies the perturbation coefficient matrix by multiplying with a PR term similar to the PR-PB-NLC technique. It is important to note that the PR method in [20] selects the optimum phase by sweeping the phase angle in the range 0 to 1 rad. On the other hand, the PR-PB-NLC technique calculates the rotation phase angle, which is proportional to the fiber effective length, as $\gamma P_0 L_{\text{eff}}$. The PR-PB-NLC can be considered as a by-product of the ERP-NLC technique by using only first part of (15). It should be noted that the additional computational complexity of the PR-PB-NLC is negligibly small when compared to the PB-NLC technique. We have included the result for the PR-PB-NLC along with the ERP-NLC technique to compare the performance. We evaluate the implementation complexity of the proposed ERP-NLC and PR-PB-NLC techniques in terms of the number of real-valued multiplications per sample in Section 5.

Fig. 1(a) shows the magnitude of $C_{m,n}$ relative to the largest coefficient $C_{0,0}$, at a transmission distance of 1200 km. The nonlinear distortion calculation in (15) contains infinite terms when m and n approach infinity. In the implementation, we truncate them when the perturbation coefficient $C_{m,n}$ is less than a threshold value given as $20 \log_{10} \left(|C_{m,n}| / |C_{0,0}| \right) < -40$ dB [14]. Fig. 1(b) shows the block diagram of the ERP-NLC technique. In the pre-compensation technique, the perturbative nonlinear distortion caused by the intra-channel nonlinearity is calculated first using (15), and then subtracted from the transmitted field, as shown in Fig. 1(b).

3. Simulation Setup

Fig. 2 shows the simulation setup for the ERP-NLC technique. At the transmitter, after the 16-QAM symbol mapping, the first-order ERP-NLC is carried out as a pre-compensation at one sample/symbol. Then, a root-raised-cosine filter with a roll-off factor 0.1 is applied in each polarization for the pulse shaping. The data transmission rate is 32 Gbaud. After digital-to-analog conversion and low-pass filtering, the pre-compensated signal is converted to optical domain using an in-phase/quadrature phase modulator. The long-haul transmission link consists of several spans of standard single-mode fiber with the span length of 80 km, the attenuation coefficient of 0.2 dB·km^{-1}, the nonlinear parameter of 1.22 W^{-1}·km^{-1}, the dispersion parameter of 16 ps·nm^{-1}·km^{-1}, and the polarization mode dispersion coefficient of 0.1 ps·km$^{-1/2}$. The optical power loss in each fiber span is compensated by an erbium doped fiber amplifier with 16 dB gain and 5.5 dB noise figure. At the receiver, the signal is coherently detected using a polarization diversity detector. After analog-to-digital conversion and root-raised-cosine filtering, dispersion compensation is performed. Then, an adaptive equalization is carried out for the state-of-polarization recovery. After that, the carrier phase is recovered using the Viterbi-Viterbi algorithm. Finally, symbol detection and demodulation is
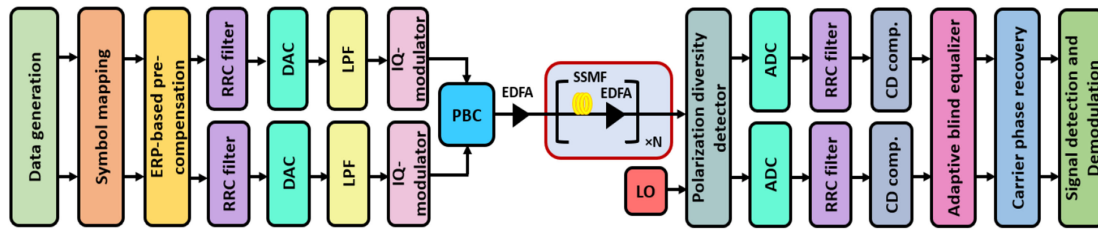
Fig. 2. Simulation setup for ERP-NLC technique (single-channel). RRC: root-raised-cosine, DAC: digital-to-analog converter, LPF: low pass filter, IQ: inphase/quadrature phase, PBC: polarization beam combiner, N: number of spans, EDFA: erbium doped fiber amplifier, ADC: analog-to-digital converter, CD: chromatic dispersion.
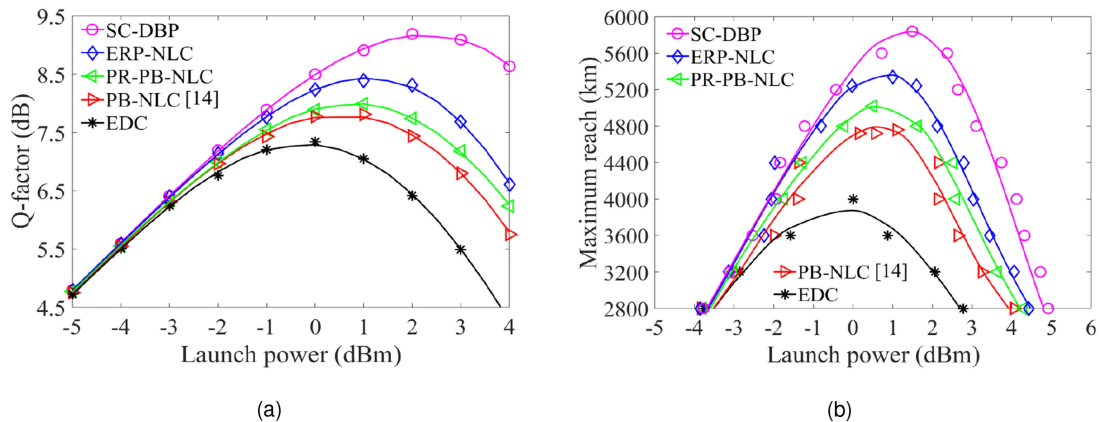

(a)   (b)

Fig. 3. The transmission performance of an SC transmission system for the SC-DBP, ERP-NLC, PR-PB-NLC, PB-NLC, and EDC techniques. (a) Q-factor versus launch power for an SC system after the propagation over 2800 km and (b) maximum reach as a function of the launch power at 20% OH-SD-FEC limit for an SC system.

applied to recover the transmitted information bits. We adopt the Q-factor to evaluate the system performance which is directly derived from the bit-error rate (BER) as $Q = 20 \log_{10}(\sqrt{2}\,\mathrm{erfc}^{-1}(2\,\mathrm{BER}))$ [21].

4. Simulation Results and Discussion

We carried out numerical simulation for the single-/five-channel polarization-division multiplexed 16-QAM optical transmission system to evaluate the performance of the proposed ERP-NLC technique. We compare the performance of the ERP-NLC technique with the single-channel (SC)-DBP, PR-PB-NLC, PB-NLC, and EDC techniques. The SC-DBP technique is implemented with one step per span. It is worth mentioning that increasing the number of steps per span increases the compensation performance of the SC-DBP technique with a corresponding increase in the computational complexity. For example, the SC-DBP with 16 steps/span can increase the optimum Q-factor by ∼1.5 dB for an SC system with a 16 times increase in the computational complexity when compared to the one step/span implementation [23]. Fig. 3 indicates the performance for a 256 Gb/s SC transmission system. It is evident from Fig. 3(a) that the proposed ERP-NLC technique improves the Q-factor performance by ∼1.2 dB and ∼0.6 dB when compared to the EDC and the PB-NLC techniques, respectively, at a transmission distance of 2800 km. It is interesting to note that the PR-PB-NLC technique improves the Q-factor by ∼0.7 dB and ∼0.2 dB when compared to the EDC and PB-NLC techniques, respectively. In Fig. 3(b), we plot the maximum reach as a function of the launch power at 20% overhead (OH) soft-decision (SD) forward error correction (FEC) limit of
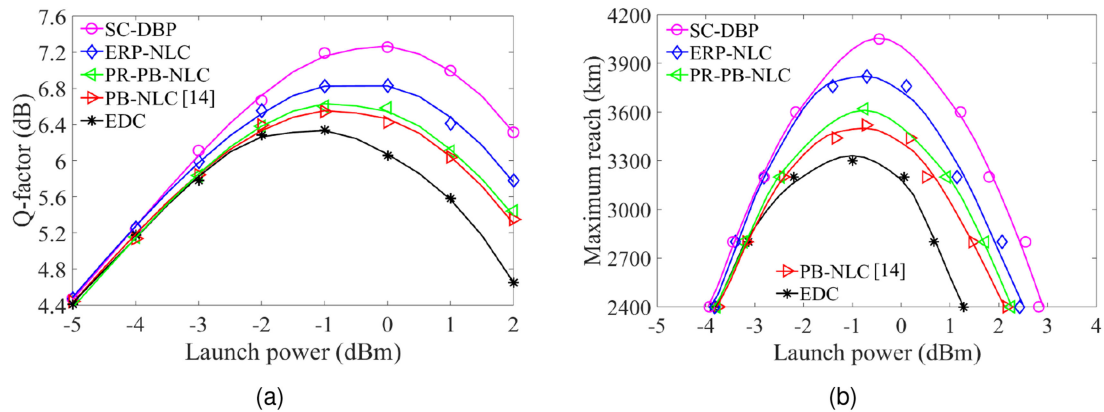
Fig. 4. The transmission performance of a five-channel WDM system for the SC-DBP, ERP-NLC, PR-PB-NLC, PB-NLC, and EDC techniques. (a) *Q*-factor versus launch power for the central WDM channel after the propagation over 2800 km and (b) maximum reach as a function of the launch power at 20% OH-SD-FEC limit for the central channel in a five-channel WDM system.

5.7 dB [22]. It is observed that the maximum transmission reach for the SC-DBP, ERP-NLC, PR-PB-NLC, PB-NLC, and EDC is 5840 km, 5340 km, 5020 km, 4760 km, and 4000 km, respectively. These results indicate that the ERP-NLC technique provides an extended transmission reach by 33.5% and 12.2% when compared to the EDC and the PB-NLC techniques, respectively. Besides the ERP-NLC technique, the PR-PB-NLC yields an extended transmission reach of 5.5% when compared to the PB-NLC technique. This is attributed to the fact that the fiber has attenuation, in reality, thereby the optimum perturbation coefficient should be different from $C_{m,n}$ of the PB-NLC technique [14]. The PR of the perturbation coefficient matrix in (14) partially solves this problem through the parameter L_{eff} in the calculated rotation phase angle of the PR-PB-NLC technique. Notably, the ERP-NLC technique improves the transmission reach by 6.4% when compared to the PR-PB-NLC technique.

The performance evaluation for a 1.28 Tb/s five-channel WDM transmission system is shown in Fig. 4. The channel spacing is 37.5 GHz. The central WDM channel is arbitrarily selected for performance evaluation. In Fig. 4(a), results show that the proposed ERP-NLC technique improves the *Q*-factor performance by ~0.6 dB and ~0.4 dB when compared to the EDC and PB-NLC techniques, respectively, at a transmission distance of 2800 km. On the other hand, the PR-PB-NLC technique shows a *Q*-factor improvement of ~0.3 dB and ~0.1 dB when compared to the EDC and PB-NLC techniques, respectively. Results given in Fig. 4(b) indicate that the maximum reach at 20% OH-SD-FEC limit for the SC-DBP, ERP-NLC, PR-PB-NLC, PB-NLC, and EDC techniques is 4050 km, 3820 km, 3620 km, 3520 km, and 3300 km respectively. Accordingly, the proposed ERP-NLC technique provides an extended transmission reach of 16%, 8.5%, and 5.5% when compared to the EDC, PB-NLC, and PR-PB-NLC techniques, respectively. In contrast, the PR-PB-NLC technique improves the transmission reach by only 2.8% when compared to the PB-NLC technique. It is observed that the *Q*-factor improvement for the WDM system is less when compared to the SC system. This can be easily explained, as the inter-channel nonlinear distortions, such as cross-phase modulation and cross-polarization modulation, are the dominant impairments in a dispersion unmanaged WDM system which cannot be compensated for by the intra-channel NLC techniques [4]. Further performance improvement can be achieved by including the inter-channel effects in the ERP-NLC technique. For WDM systems with many channels, the strong walk-off and phase-mismatch between the widely separated channels reduce the nonlinearity effects on transmission beyond an effective bandwidth [23]. In such cases, a mean field approach can be used for NLC, which neglects the time and *z*-variations of the channels outside an effective bandwidth [23]. The effective bandwidth is chosen as a trade-off between implementation complexity and compensation performance [23].
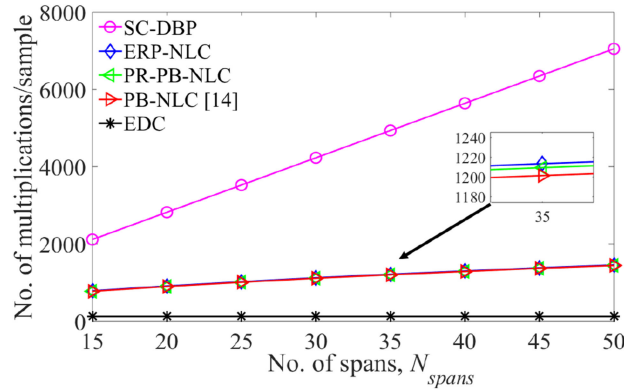
Fig. 5. The number of real-valued multiplications/sample for the SC-DBP, ERP-NLC, PR-PB-NLC, PB-NLC, and EDC techniques as a function of the number of spans.

5. Complexity Evaluation

In this section, the computational complexity evaluation is performed for the SC-DBP, ERP-NLC, PR-PB-NLC, PB-NLC, and EDC techniques; the real-valued multiplications per sample is considered as performance metric. SC-DBP is implemented with one step per span. The nonlinearity coefficient matrix of the ERP/RP-based NLC techniques is truncated at a threshold of -40 dB. Number of real-valued multiplications per sample for SC-DBP is given by $2(4N_{spans}N_{\text{FFT}} \log_2(N_{\text{FFT}}) + 10.5N_{spans}N_{\text{FFT}})/N_s$, where N_{spans} is the number of fiber spans, N_{FFT} is the fast Fourier transform size, and N_s is the number of samples [7]. For the PB-NLC technique, the expression for the number of real-valued multiplications per sample is given as $2(20M + 3)$, where M is the number of significant perturbation coefficients in $C_{m,n}$ [24]. In the PR-PB-NLC technique, the phase rotation term $\exp(-j\gamma P_0 L_{\text{eff}})$ is calculated offline and stored in look-up table. Accordingly, the PR-PB-NLC technique has only one additional complex-valued multiplication per sample when compared to the PB-NLC technique. Therefore, the number of real-valued multiplications per sample for the PR-PB-NLC technique is given as $2(20M + 7)$. The proposed ERP-NLC technique consists of an additional time-invariant phase rotation term $\exp(-j\gamma P_0 L_{\text{eff}})$ and a time-variant term $P_0 A_{0,x/y} L_{\text{eff}}$ when compared to the PB-NLC technique. It is important to note that the phase rotation term $\exp(-j\gamma P_0 L_{\text{eff}})$ is calculated offline and stored in look-up table, as in the PR-PB-NLC technique. That yields only one complex-valued multiplication per sample in the implementation of the ERP-NLC technique. Similarly, the term $P_0 A_{0,x/y} L_{\text{eff}}$ contributes two real-valued multiplications and one complex-valued multiplication per sample to the computational complexity of the ERP-NLC technique. As a result, the number of real-valued multiplications per sample for the ERP-NLC technique is given as $2(20M + 9)$. For the EDC technique, the number of real-valued multiplications per sample is given as $2(4N_{\text{FFT}} \log_2(N_{\text{FFT}}) + 4N_{\text{FFT}})$ [7]. It is important to note that the factor 2 in the complexity expressions accounts for the dual polarization transmission.

Fig. 5 shows the number of real-valued multiplications per sample as a function of the number of fiber spans, N_{spans} for the considered techniques. Results show that the complexity of the SC-DBP technique increases rapidly as the number of fiber span increases. On the other hand, for the ERP-NLC, PR-PB-NLC, and PB-NLC techniques, the complexity increases only slightly as the number of fiber spans increases. This is due to a slight increase in the number of coefficients in the nonlinear coefficient matrix $C_{m,n}$, satisfying the truncation threshold, as the number of fiber spans increases. It is interesting to note that the additional computational complexity of the ERP-NLC and PR-PB-NLC techniques, when compared to the PB-NLC technique, is negligible.

6. Conclusion

In this paper, we have proposed an ERP-based NLC technique, referred to as ERP-NLC. We have shown through numerical simulations that this technique extends the transmission reach by 33.5%, 12.2%, and 6.4% when compared to the EDC, PB-NLC, and PR-PB-NLC techniques, respectively, for a 256 Gb/s single-channel transmission system. We have also demonstrated that, for a 1.28 Tb/s five-channel WDM transmission system, ERP-NLC improves the transmission reach by 16%, 8.5%, and 5.5% when compared to the EDC, PB-NLC, and PR-PB-NLC techniques, respectively. The complexity evaluation using the number of real-valued multiplications per sample indicates that the additional complexity of the proposed ERP-NLC technique is negligibly small when compared to the PB-NLC technique.

Appendix A
First-Order ERP-Based Distortion Calculation

In Section 2.1, we obtained the first-order ERP-based solution by applying a change of variable technique in (2) to solve the energy divergence problem of the RP-based method. Equation (10) represents the first-order ERP distortion field in time-domain. By taking the Fourier transform of (10), we get the distortion field in frequency-domain at a transmission distance $z = L$ as:

$$U_1^{ERP}(L, w) = j\gamma \int_0^L \tilde{F}(z, w) \exp\left(-j\frac{w^2 \beta_2 z}{2}\right) \exp(-\alpha z)dz, \tag{16}$$

where $\tilde{F}(z, w)$ is given as:

$$\tilde{F}(z, w) = \mathcal{F}\{[|\tilde{u}_0(z, t)|^2 \tilde{u}_0(z, t) - P_0\tilde{u}_0(z, t)]\exp(-j\gamma P_0 L_{eff})\}. \tag{17}$$

The input field to the optical fiber can be represented as:

$$\tilde{u}(z = 0, t) = \sqrt{P}\sum_k A_k \tilde{g}(z = 0, t - kT) = \sqrt{P}\sum_k A_k \tilde{g}(0, k), \tag{18}$$

where P is the launch power, A_k is the symbol complex amplitude imposed by data modulation on the kth pulse, $\tilde{g}(z, t)$ is the pulse temporal waveform, and T is the symbol interval. By substituting (18) in (17) and calculating the FT, we obtain:

$$\tilde{F}(z, w) = P^{3/2}\sum_m\sum_n\sum_l A_m A_n A_l^*[\tilde{G}_m(z, w) \otimes \tilde{G}_l^*(z, -w) \otimes \tilde{G}_n(z, w)$$
$$- P_0 A_k \tilde{G}(z, w)]\exp(-j\gamma P_0 L_{eff}), \tag{19}$$

where $*$ is the complex conjugation operation, m, n, l are the symbol indices, and $\tilde{G}(z, w) = \mathcal{F}\{\tilde{g}(z, t)\}$. Calculating the convolution operation in (19) and substituting the result in (16), we get the ERP kernel term in frequency-domain as:

$$U_1^{ERP}(L, w) = \underbrace{\begin{pmatrix} j\gamma A_m A_l^* A_n \int_0^L \int\int \exp(-\alpha z)\tilde{G}(0, w_1 + w)\tilde{G}^*(0, w_1 + w - w_2)\tilde{G}(0, w - w_2) \\ \times \exp(-j[w_1(T_m - T_l) + w_2(T_l - T_n) - \beta_2 z w_1 w_2])dw_1 dw_2 dz \\ \times \exp(-jw(T_m + T_n - T_l))\exp(-j\gamma P_0 L_{eff}) \end{pmatrix}}_{\text{term 1}}$$

$$\underbrace{- j\gamma P_0 A_k \int_0^L \exp(-\alpha z)\tilde{G}(0, w)dz \exp(-j\gamma P_0 L_{eff})}_{\text{term 2}}. \tag{20}$$

The ERP kernel in time-domain can be obtained by calculating the IFT of (20). First, we consider term 1 and calculate the IFT. Assuming the Gaussian shape for input pulses, i.e., $\tilde{G}(0, w) = \sqrt{2\pi\tau^2}\exp(-\frac{w^2\tau^2}{2})$, with τ as the pulse width, the product of the triplet pulses in term

1 can be represented as [14]:

$$\tilde{G}(0, w_1 + w)\tilde{G}^*(0, w_1 + w - w_2)\tilde{G}(0, w - w_2) = \left(\sqrt{2\pi\tau^2}\right)^3 \exp\left(-\frac{3\tau^2 w^2}{2}\right)$$

$$\times \exp(-\tau^2[w_1^2 + w_2^2 + 2(w_1 - w_2)w - w_1 w_2]). \quad (21)$$

Substituting (21) in term 1 of (20) and following a similar procedure with the phase matching condition $m + n - l = k$, as in [14], the IFT of term 1 is obtained as:

$$\tilde{u}_{1,\text{term 1}}^{ERP}(L, t + kT) = j\gamma P^{3/2} \exp(-j\gamma P_0 L_{\text{eff}}) \sum_m \sum_n \sum_l A_m A_n A_l^*$$

$$\times \exp\left(-\frac{t^2}{6\tau^2}\right) \int_0^L \frac{\exp(-\alpha z)}{\sqrt{1 + 2j\beta_2 z/\tau^2 + 3(\beta_2 z/\tau^2)^2}}$$

$$\times \exp\left\{ -\frac{3\left[\frac{2}{3}t + (m-l)T\right]\left[\frac{2}{3}t + (n-l)T\right]}{\tau^2\left(1 + 3j\beta_2 z/\tau^2\right)} - \frac{(n-m)^2 T^2}{\tau^2\left[1 + 2j\beta_2 z/\tau^2 + 3(\beta_2 z/\tau^2)^2\right]} \right\} dz. \quad (22)$$

Next, consider term 2 and calculate the IFT as:

$$\tilde{u}_{1,\text{term 2}}^{ERP}(L, t + kT) = j\gamma \sqrt{2\pi\tau^2} P_0 A_k \int_0^L \int \exp(-\alpha z) \exp\left(-\frac{w^2\tau^2}{2}\right) dz \exp(-j\gamma P_0 L_{\text{eff}}) \exp(jwt) dw\, dz$$

$$= j\gamma P_0 A_k \exp\left(-\frac{t^2}{2\tau^2}\right) \int_0^L \exp(-\alpha z) \exp(-j\gamma P_0 L_{\text{eff}}) dz. \quad (23)$$

Combining (22) and (23), the first-order ERP kernel term in time-domain can be represented as:

$$u_1^{ERP}(L, t + kT) = \tilde{u}_{1,\text{term 1}}^{ERP}(L, t + kT) - \tilde{u}_{1,\text{term 2}}^{ERP}(L, t + kT). \quad (24)$$

Appendix B
Extension to Dual Polarization

In the dual polarization case, the electric field input to the optical fiber is a column vector $\mathbf{u}(z, t) = [u_x(z, t)\ u_y(z, t)]^\dagger$, with x, y representing the horizontal and vertical polarization, respectively, and the superscript $\dagger$ as the transpose. The propagation of the vector field $\mathbf{u}(z, t)$ through the optical fiber can be represented using the Manakov equation, where the nonlinear effective length is much longer than the fiber birefringent beating length, as [14]:

$$\frac{\partial}{\partial z}\mathbf{u} + j\frac{\beta_2}{2}\frac{\partial^2}{\partial t^2}\mathbf{u} = j\frac{8}{9}\gamma(\mathbf{u}^{*\dagger}\mathbf{u}\mathbf{I})\mathbf{u}, \quad (25)$$

where $\mathbf{I}$ is the identity matrix. Note that in (25), we omitted the space and time variables z, t for the sake of simplicity. After applying the change of variable technique, as in the single polarization case, the modified Manakov equation can be represented as:

$$\frac{\partial}{\partial z}\tilde{\mathbf{u}} + j\frac{\beta_2}{2}\frac{\partial^2}{\partial t^2}\tilde{\mathbf{u}} = j\frac{8}{9}\gamma(\tilde{\mathbf{u}}^{*\dagger}\tilde{\mathbf{u}}\mathbf{I} - P_0\mathbf{I})\tilde{\mathbf{u}}, \quad (26)$$

where $\tilde{\mathbf{u}}(z, t) = [\tilde{u}_x(z, t)\ \tilde{u}_y(z, t)]^\dagger$. After solving (26) with the ERP technique, the zeroth- and first-order solutions for the output field can be represented as:

$$u_{0,x/y}^{ERP}(L, t) = \tilde{u}_{0,x/y}(L, t) \exp(-j\gamma P_0 L_{\text{eff}}) \quad (27)$$

and

$$u_{1,x/y}^{ERP}(L, t) = j\frac{8}{9}\gamma \int_0^L \exp(-\alpha z) \left(h_L(t) \otimes \left[\left(\left| \tilde{u}_{0,x/y}(z, t) \right|^2 - P_0 \right) \tilde{u}_{0,x/y}(z, t) \right] \right) dz$$
$$\times \exp(-j\gamma P_0 L_{\text{eff}}). \tag{28}$$

References

[1] M. Malekiha *et al.*, "Efficient nonlinear equalizer for intra-channel nonlinearity compensation for next generation agile and dynamically reconfigurable optical networks," *Opt. Exp.*, vol. 24, no. 4, pp. 4097–4108, Feb. 2016.

[2] O. S. Sunish Kumar, A. Amari, O. A. Dobre, and R. Venkatesan, "PDL impact on linearly coded digital phase conjugation techniques in CO-OFDM systems," *IEEE Photon. Technol. Lett.*, vol. 30, no. 9, pp. 769–772, May 2018.

[3] X. Liang and S. Kumar, "Correlated digital back propagation based on perturbation theory," *Opt. Exp.*, vol. 23, no. 11, pp. 14655–14665, May 2015.

[4] O. Vassilieva, I. Kim, and T. Ikeuchi, "Enabling technologies for fiber nonlinearity mitigation in high capacity transmission systems," *J. Lightw. Technol.*, vol. 37, no. 1, pp. 50–60, Jan. 2019.

[5] A. Amari, O. A. Dobre, R. Venkatesan, O. S. S. Kumar, P. Ciblat, and Y. Jaouën, "A survey on fiber nonlinearity compensation for 400 Gb/s and beyond optical communication systems," *IEEE Commun. Surv. Tut.*, vol. 19, no. 4, pp. 3097–3113, Oct.–Dec. 2017.

[6] F. P. Guiomar, J. D. Reis, A. L. Teixeira, and A. N. Pinto, "Digital postcompensation using Volterra series transfer function," *IEEE Photon. Technol. Lett.*, vol. 23, no. 19, pp. 1412–1414, Oct. 2011.

[7] A. Amari, O. A. Dobre, and R. Venkatesan, "Fifth-order Volterra series based nonlinear equalizer for long-haul high data rate optical fiber communications," in *Proc. IEEE Int. Conf. Transparent Opt. Netw.*, Jan. 2017, Paper We.A1.2.

[8] V. Vgenopoulou *et al.*, "Volterra-based nonlinear compensation in 400 Gb/s WDM multiband coherent optical OFDM systems," in *Proc. Asia Commun. Photon. Conf.*, Nov. 2014, Paper AF1E. 4.

[9] E. P. Silva, M. P. Yankov, F. Da Ros, T. Morioka, and L. K. Oxenlwe, "Perturbation-based FEC-assisted iterative nonlinearity compensation for WDM systems," *J. Lightw. Technol.*, vol. 37, no. 3, pp. 875–881, Feb. 2019.

[10] A. Ghazisaeidi *et al.*, "Perturbative nonlinear pre-compensation in presence of optical filtering," in *Proc. Opt. Fiber Commun. Conf.*, Mar. 2015, Paper ThD3.3.

[11] T. Oyama *et al.*, "Robust and efficient receiver-side compensation method for intra-channel nonlinear effects," in *Proc. Opt. Fiber Commun. Conf.*, Mar. 2014, Paper Tu3A.3.

[12] Y. Gao *et al.*, "Joint pre-compensation and selective post-compensation for fiber nonlinearities," *IEEE Photon. Technol. Lett.*, vol. 26, no. 17, p. 1746–1749, Jun. 2014.

[13] A. Mecozzi, C. B. Clausen, and M. Shtaif, "Analysis of intrachannel nonlinear effects in highly dispersed optical pulse transmission," *IEEE Photon. Technol. Lett.*, vol. 12, no. 4, pp. 392–394, Apr. 2000.

[14] Z. Tao, L. Dou, W. Yan, L. Li, T. Hoshida, and J. C. Rasmussen, "Multiplier-free intrachannel nonlinearity compensating algorithm operating at symbol rate," *J. Lightw. Technol.*, vol. 29, no. 17, pp. 2570–2576, Sep. 2011.

[15] A. Vannucci, P. Serena, and A. Bononi, "The RP method: A new tool for the iterative solution of the nonlinear Schrdinger equation," *J. Lightw. Technol.*, vol. 20, no. 7, pp. 1102–1112, Jul. 2002.

[16] P. Serena and A. Bononi, "An alternative approach to the Gaussian noise model and its system implications," *J. Lightw. Technol.*, vol. 31, no. 22, pp. 3489–3499, Nov. 2013.

[17] G. P. Agrawal, *Nonlinear Fiber Optics.* San Diego, CA, USA: Academic, 1995.

[18] E. Ip and J. M. Kahn, "Compensation of dispersion and nonlinear impairments using digital backpropagation," *J. Lightw. Technol.*, vol. 26, no. 20, pp. 3416–3425, Oct. 2008.

[19] B. R. Washburn, "Dispersion and nonlinearities associated with supercontinuum generation in microstructure fibers," Ph.D dissertation, School of Physics, Georgia Inst. Technol., Atlanta, GA, USA, 2005.

[20] L. Dou *et al.*, "Pre-distortion method for intra-channel nonlinearity compensation with phase-rotated perturbation term," in *Proc. Opt. Fiber Commun. Conf.*, Mar. 2012, Paper OTh3C.2.

[21] O. S. Sunish Kumar *et al.*, "A spectrally-efficient linear polarization coding scheme for fiber nonlinearity compensation in CO-OFDM systems," *Proc. SPIE Opt.*, vol. 10130, Jan. 2017, Art. no. 101300P.

[22] O. S. Sunish Kumar *et al.*, "A joint technique for nonlinearity compensation in CO-OFDM superchannel systems," in *Proc. Asia Commun. Photon. Conf.*, Nov. 2017, Paper Su4B.4.

[23] E. Mateo *et al.*, "Impact of XPM and FWM on the digital implementation of impairment compensation for WDM transmission using backward propagation," *Opt. Exp.*, vol. 16, no. 20, pp. 16124–16137, Sep. 2008.

[24] X. Liang and S. Kumar, "Multi-stage perturbation theory for compensating intra-channel nonlinear impairments in fiber-optic links," *Opt. Exp.*, vol. 22, no. 24, pp. 29733–29745, Nov. 2014.